Static structure and colloidal interactions in partially quenched quasibidimensional colloidal mixtures

G. Cruz de León and J. L. Arauz-Lara
Instituto de Física ''Manuel Sandoval Vallarta,'' Universidad Autónoma de San Luis Potosí, Alvaro Obregón 64, 78000 San Luis Potosí, SLP, Mexico
(Received 10 September 1998)

Partially quenched quasibidimensional colloidal suspensions are obtained by confining a bidisperse aqueous suspension of polystyrene spheres between two glass plates. The larger particles are fixed between the plates, forming a disordered bidimensional matrix of obstacles, with respect to which the colloidal suspension of the smaller species of particles equilibrates. Digital video microscopy is used to measure the static structure of both the colloidal suspension and the matrix for various fixed particles concentrations. The effective pair potentials between the mobile particles $u_{11}(r)$ and between mobile and fixed particles $u_{12}(r)$ are obtained by deconvoluting the structural information of the system via the Ornstein-Zernike equation. The measured pair potential $u_{11}(r)$ exhibits two attractive components. One of them, at intermediate distances, is present at all fixed particle concentrations, while the second one, of longer range, develops as the number of obstacles increases. The pair potential $u_{12}(r)$ also has an attractive component at intermediate distances. [S1063-651X(99)10503-8]

PACS number(s): 82.70.Dd, 05.40.−a, 47.55.Mh

I. INTRODUCTION

In many natural and industrial processes one is concerned with the description of fluid systems permeating a porous matrix. Most of the interest in such systems is due to their technological relevance which spans a wide range of applications [1,2]. A microscopic understanding of the physical properties of the permeating fluid, such as its structure, dynamics, thermodynamics, etc., requires the accurate determination of the interactions between the fluid particles and between them and the matrix, as well as detailed information on the matrix structure, morphology, porosity, etc. However, in most cases such complete information of the system is not available, mainly due to the complexity of naturally occurring porous materials. On the other hand, suitable theoretical models of porous media have been introduced in the literature, which allow to test theoretical tools for the description of the matrix and the properties of absorbed fluids. Of particular interest, it is the model of a partially quenched fluid mixture. This model consists of a binary mixture, where the particles of one species are frozen in a given configuration while the other species equilibrates in the static field of the frozen matrix and represent the fluid phase. To study these type of systems with quenched disorder, extensions of the liquid theory methods have been developed to characterize the static structure of both the liquid phase and the structure of the solid matrix in terms of quantities such as the two-body correlation functions, where the interaction potentials between the mobile particles and between mobile and fixed particles are given, as well as the fixed particle configuration [3–5]. Computer simulation methods have also been implemented to consider both the static structure and dynamics of the mobile species [6,7].

Here, we study a colloidal system that is a quasibidimensional experimental realization of the model discussed above. The system consists of a binary mixture of polystyrene spheres of diameters σ_1 and σ_2, with $\sigma_2 > \sigma_1$, suspended in water. The suspension is confined between two glass plates, in such a way that the separation between the inner surfaces of the plates coincides with σ_2. Thus, the dynamics of the species 2 is quenched, i.e., the particles of species 2 are frozen in a disordered configuration forming in this way a two-dimensional (2D) (porous) matrix of fixed particles. The particles of species 1 form then an effective 2D colloidal fluid which equilibrates in the field of the fixed particles of species 2. The particles of the species 1 are fluorescent polystyrene spheres of diameter 0.5 μm, and the particles of species 2 are nonfluorescent polystyrene spheres of diameter 2.05 μm. The differences in size and in color of both species, allow us to clearly identify the particles of the different species and to determine accurately their positions using digital video microscopy (DVM). In Sec. II we describe in more detail the sample preparation and data analysis.

The structure of the colloidal fluid, characterized by the radial distribution function $g_{11}(r)$ of the diffusing particles, is measured for different concentrations of fixed particles keeping fixed the mobile particle's concentration. In this way we measure the structural changes of the colloidal suspension as the porosity of the matrix is reduced. This system allow us also to measure other quantities of interest which complement the structural information of the system, namely, the fluid-solid correlation function $g_{12}(r)$, and the structure of the matrix given by the correlation function between fixed particles $g_{22}(r)$. Contrary to the theoretical models where one assumes the interparticle potentials, in real systems the effective pair interaction potentials have to be determined experimentally. For the case of homogeneous three-dimensional (3D) aqueous suspensions of polystyrene spheres, the assumption of a repulsive screened Coulomb effective pair potential, as the one derived by Derjaguin, Landau, Verwey, and Overbeek (DLVO) [8], provides a functional form for the interparticle potential in terms of which the experimental observations have been reasonably

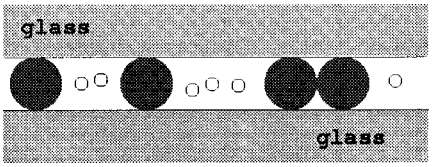

FIG. 1. Schematic representation of the side view of a sample. The dark circles represent the fixed particles of species 2, while the open smaller circles the mobile particles of species 1.

well described [9,10]. However, for the same kind of systems but now confined between two parallel glass plates, direct and indirect determinations of the effective interparticle potential show an attractive component, rather than repulsive, at intermediate distances [11–13]. For the systems considered here, such attractive interaction becomes of larger range as the concentration of fixed particles increase. This observation, reported in a previous paper [14], is presented here in more detail, together with the interaction potential between mobile and fixed particles. Those effective pair potentials are determined by deconvoluting the information contained in the measured structural properties of the system, by using the multicomponent Ornstein-Zernike (OZ) integral equation and a closure relation. In Sec. III, we present the measured structural properties of the system and the effective pair potentials. A discussion of our results and the conclusions are given in Sec. IV.

II. EXPERIMENTAL DETAILS

A. System preparation

Colloidal suspensions of fluorescent polystyrene spheres of diameter $\sigma_1 = 0.5 \pm 0.015$ μm and nonfluorescent polystyrene spheres of diameter $\sigma_2 = 2.05 \pm 0.05$ μm (Duke Scientific) are diluted in ultrapure water and dialyzed to reduce the ionic concentration and the excess of surfactants from the original batches. The systems studied are prepared as follows: in a clean atmosphere of nitrogen gas, both suspensions are mixed together at different proportions to produce binary colloidal mixtures with different concentrations of large particles, but with constant concentration of particles of species 1. A tiny volume of the mixture (≈ 0.5 μl), is confined between two carefully cleaned glass plates (a slide and a cover slip) which are uniformly pressed one against the other until the motion of the large particles is totally quenched. This occurs when the separation between the plates coincides with σ_2. Thus, the large particles are frozen in a disordered configuration forming a matrix of fixed obstacles, or porous matrix, while the smaller species form a suspension of mobile particles that permeates this matrix. The system is sealed with epoxy resin (Epo-Tek 302) to avoid any further contamination, especially from airborne CO_2. By carefully controlling the volume of suspension used in each sample, we avoid the contact with the epoxy resin and this prevents any contamination from the solvents. The sample is allowed to equilibrate for 1 or 2 days at a constant temperature of 25 °C (in contact with a circulating bath). The systems prepared with this procedure remain stable for several weeks or even several months. Figure 1 shows a schematic representation of a sample as it is seen from a side view.

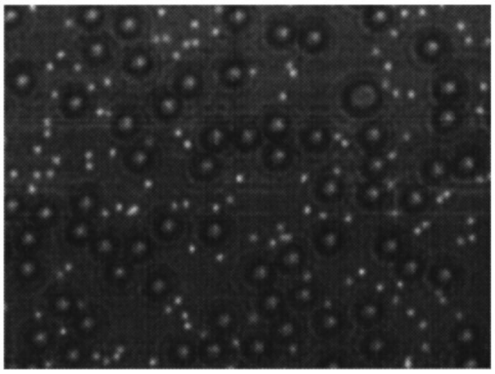

FIG. 2. Image of a sample taken using fluorescent and transmitted light illumination, and a 100× objective. Here both the mobile (bright) and fixed (shadow) particles are clearly imaged. The scale of the picture is 60 μm along the x direction.

B. Digital video microscopy

The basic components of digital video microscopy are, as it is setup in our laboratory, a fluorescence microscope (Zeiss Axioskop), a CCD video camera with a shutter exposure time of 1/250 sec, a video tape recorder (Hi8 Sony EV-100), and a frame grabber with a resolution of 640 $\times$480 pixel^2 (Data Translation). We observe the samples using a 100× oil immersion objective (numerical aperture of 1.3), and a 40× objective (numerical aperture of 0.75), as we explain below. For illustration, in Figs. 2 and 3 we show typical images of one of the samples studied here as it seen using the 100× and the 40× objectives, respectively. The picture in Fig. 2 was taken using transmitted and fluorescence illumination. This increase the optical contrast between the particles, and allows to distinguish one species from the other. The small and bright particles are the fluorescent particles of species 1, and the larger and shadow particles are the fixed particles. Figure 3 shows the same sample, at lower magnification, using only transmitted light. Here, only the fixed particles are clearly imaged, showing a typical configuration of the porous matrix at a larger scale.

C. Data analysis

The pair correlation functions $g_{ij}(r)$ are determined from the positions of the particles [12,15], which are obtained

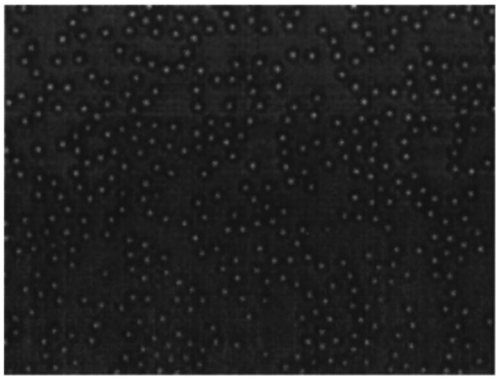

FIG. 3. Image of the sample in Fig. 2 at lower magnification, taken using a 40× objective and transmitted light. Here only the larger particles are clearly imaged. The scale of the picture is 122 μm along the x direction.

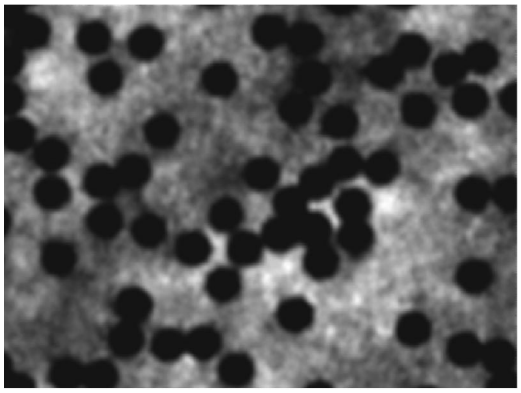

FIG. 4. A superposition of 1000 images of different mobile particles configurations, taken at the same matrix location. The bright and dark areas represent the accessible and unreachable space to the mobile colloidal particles, respectively.

from the digitized images by using the method deviced by Crocker and Grier [16]. This method allows to locate the spheres' centroids with a precision of 1/5 pixel. With our setup we measure 1 μm=16.7 and 8.2 pixels, with the 100× and 40× objectives, respectively. For the determination of $g_{11}(r)$ and $g_{12}(r)$, we observe the sample with the 100× objective and digitized 3600 different mobile particles configurations at various sites of the sample, i.e., at various fixed particles configurations, as the one shown in Fig. 2. In practice, to avoid confusions, we identify the particles of both species at the same location separately. For this, we use the difference in size of both species, and the fact that the mobile particles are fluorescent and the fixed particles are nonfluorescent, in the following way. We first observe the sample using fluorescence illumination to see only the particles of species 1. Then, we observe the sample with transmitted light and we focus at the top of the larger particles so that only these particles are clearly imaged. In this way we clearly identify both species independently. To determine $g_{22}(r)$, i.e., the structure of the matrix of fixed particles, we digitized images at several ($\sim$2000) different locations of the sample, using transmitted light and the 40× objective (see Fig. 3). The lower magnification allow us to determine the structure of the matrix with data obtained at a larger spatial scale. To end this section, let us mention that one important parameter in the characterization of porous media is the effective space available to the fluid phase. In our systems we can determine this parameter in a very simple way. Figure 4 shows a superposition of 1000 images of the mobile particles at one location of the sample using only fluorescence illumination. Here one can see the effective space available to the mobile particles, the white area, as well as the unreachable dark area, which in the case shown here it corresponds mainly to the area determined by the presence of the fixed particles.

III. RESULTS AND DISCUSSION

A. Static structure

The physical quantities describing how the mobile particles locally structure around a mobile particle and around a fixed particle are the pair correlation functions $g_{11}(r)$ and $g_{12}(r)$, respectively. For the kind of systems studied here,

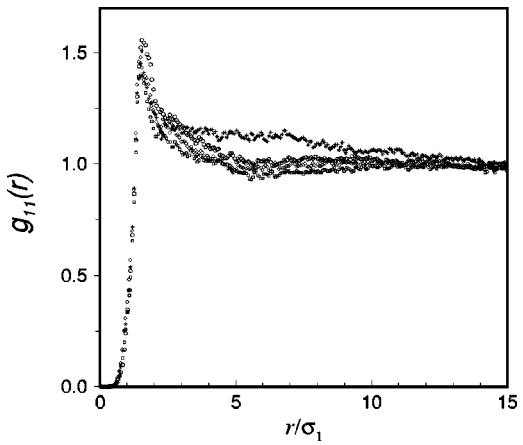

FIG. 5. Radial distribution function of the mobile particles measured at 4 different configurations of fixed particles. In this sample $n_1^*=0.02$ and $n_2^*=0.25$. Different symbols represent measurements at different sites.

where one species is fixed in a disordered configuration, those pair correlation functions are expected to depend to some extent on the local configuration of fixed particles where they are measured. Thus, the measurement of $g_{11}(r)$ and $g_{12}(r)$ at different sites on each sample should provide information of such dependence, as well as on the common features. To illustrate this, in Figs. 5 and 6 we show $g_{11}(r)$ and $g_{12}(r)$, respectively, measured at 4 different sites on a sample with mobile and fixed particles reduced concentration $n_1^*=0.02$ and $n_2^*=0.25$. Here $n_i^*\equiv n_i\sigma_i^2$, where $n_i=N_i/A$ is the average concentration of particles of species i, with N_i being the average number of particles of species i in a frame of area A. Different symbols represent the correlation functions at different sites on the sample, determined from 3600 different configurations of the mobile particles at each site. As shown in these figures, at short distances the structure of the mobile particles exhibits a qualitative behavior nearly independent of the local fixed particles configuration, while at larger distances the local effect of the matrix become more apparent. An average of $g_{11}(r)$, and $g_{12}(r)$, measured at different sites, would average out local effects leaving only the common behavior, which represents then the general

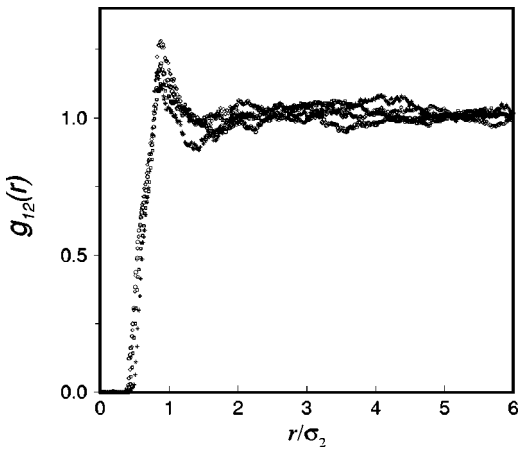

FIG. 6. Cross-correlation function measured at the same sites as $g_{11}(r)$ in Fig. 5.

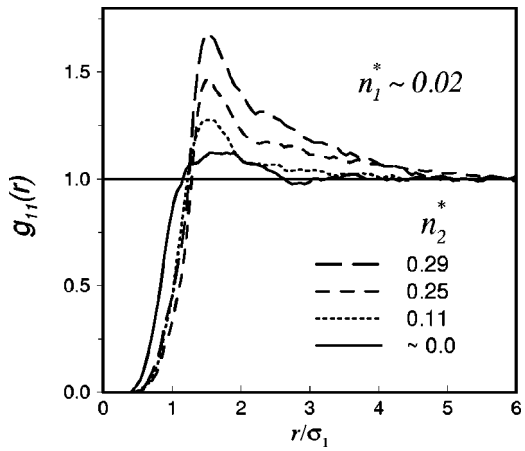

FIG. 7. Matrix-averaged radial distribution function of the mobile particles at various concentrations of the fixed particles.

physical characteristics of the system. In the following, we will show the average of 4 measurements of those functions.

Figure 7 shows $g_{11}(r)$ for various concentrations of fixed particles. In order to minimize the effect of the interactions between the mobile particles on the pair correlation functions $g_{ij}(r)$, we kept the average particle concentration of species 1, n_1, very low. In all our samples the reduced concentration n_1^* was ≈ 0.02. Thus, in Fig. 7 one can see the effect of the porous matrix on the structure of the colloidal fluid. In the limit of very low concentrations of fixed particles ($n_2^* \approx 0$), the system corresponds to a monodisperse quasi-bidimensional suspension. Here the few large particles present in the system serve only as spacers and allow us to control accurately the distance between the plates. Since the colloidal suspension is rather dilute, the measured $g_{11}(r)$ exhibits only a low first peak (solid line), at around $r = 1.5\sigma_1$, followed by minor oscillations that fade away rather quickly. At finite values of n_2^*, $g_{11}(r)$ reveals an increase in the structure of the colloidal fluid. As one can see here, the height of the first peak of $g_{11}(r)$ increases quite appreciably as n_2^* increases and, interestingly, its position is almost independent of n_2^*. One can also notice in Fig. 7 that the first peak of $g_{11}(r)$ decays more slowly for larger values of n_2^* and that there is an abrupt change in the slope that, also interestingly, happens at the same place (around $r = 2.2\sigma$) in all the samples. This behavior of $g_{11}(r)$ is different from what it is observed in homogeneous suspensions, i.e., when instead of increasing the number of frozen particles, one varies n_1^* keeping $n_2^* \approx 0$. In this case, the system is an effective 2D system that can be considered homogeneous along the plane parallel to the plates [12,17]. There, as the particle concentration increases, the radial distribution function develops a higher first maximum, followed by a minimum, a lower secondary maximum, and so on. The positions of the maxima and minima depend on concentration and there are not abrupt changes in the slope of the radial distribution function [12]. Thus, the presence of fixed obstacles, or porous matrix, enhances the correlation between the mobile particles, but there is not any development of secondary maxima or minima, as it is the case for homogeneous systems. Here the correlations become stronger and of longer range, but $g_{11}(r)$ has basically only one peak that

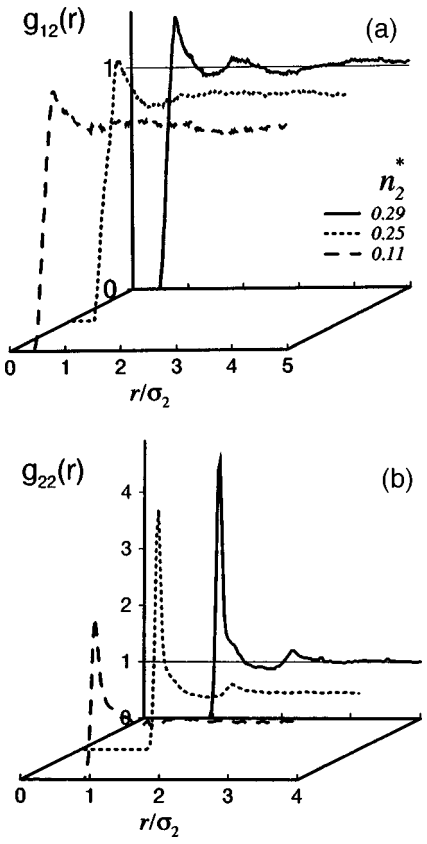

FIG. 8. Matrix-averaged cross correlation function (a) and fixed particles' radial distribution function (b) for the systems in Fig. 7.

decays slower for larger values of n_2^* and exhibits a marked change in the slope.

The cross-correlation functions between fixed and mobile particles, $g_{12}(r)$, are shown in Fig. 8(a). An interesting feature to be noticed here is the existence of a low first maximum of $g_{12}(r)$ with height and position varying very little with n_2^*. Another effect of increasing the number of fixed particles, is the development of long range correlations between the particles of species 1 and 2, exhibited in the presence of more evident oscillations of $g_{12}(r)$ at longer distances as n_2^* increases. For the particles of species 2, we can also determine the corresponding radial distribution function, $g_{22}(r)$, as a practical way to characterize the structure of the porous matrix. Thus, in Fig. 8(b) we show $g_{22}(r)$ for the same systems. These curves were determined from $(1-2) \times 10^3$ different configurations of the fixed particles, i.e., from images taken at different sites on the sample, using the 40 $\times$ objective, as the one shown in Fig. 3. In all of these samples, $g_{22}(r)$ has a very high first maximum close to contact. For the larger values of n_2^*, one can observe the development of a minimum and a secondary maximum. This shape of $g_{22}(r)$ resembles a system of hard disks, although in our systems the first peak is much higher than that corresponding to a hard disk system at the same particle concentration. Since the particle concentration of the colloidal fluid is kept low, their influence on the structure of the fixed particles is expected to be negligible.

B. Colloidal interactions

The interparticle interactions are the fundamental quantities determining colloidal properties such as stability, struc-

ture, dynamics, thermodynamics, and so on. As mentioned before, experimental data [11–14] and recent theoretical calculations [19] support the notion of a dramatic change in the pair potential between charged particles under some conditions of confinement, as compared with the interaction of the same particles in the bulk. In this section, we describe in some detail the method employed to determine the effective interaction potential between mobile particles and between them and the fixed particles, i.e., the matrix. These potentials can be extracted from the detailed structural information of the system contained in $g_{ij}(r)$, by deconvoluting this information via the 2D Ornstein-Zernike integral equation. For multicomponent systems, the O-Z equation is a set of coupled integral equations for the total correlation functions $h_{ij}(r)=g_{ij}(r)-1$ $(i,j=1,2,\ldots,m)$ where m is the number of species in the system. The set of equations in 2D reads

$$h_{ij}(r)=c_{ij}(r)+\sum_{k=1}^{m} n_k \int d^2r' c_{ik}(r')h_{kj}(|\mathbf{r}-\mathbf{r}'|), \tag{3.1}$$

where $c_{ij}(r)$ are the direct correlation functions between particles of species i and j, n_k is the 2D particle concentration of species k. For symmetry, we assume $h_{ji}(r)=h_{ij}(r)$ and $c_{ji}(r)=c_{ij}(r)$. Usually the O-Z equation is employed to calculate $g_{ij}(r)$ assuming known the pair potentials $u_{ij}(r)$ between the different species. In these equations both sets of functions $h_{ij}(r)$ and $c_{ij}(r)$ are unknown functions. Therefore, an additional set of relations are required to be able to solve Eq. (3.1) to obtain the system's structural information, i.e., $g_{ij}(r)$. Closure relations to Eq. (3.1) have been introduced in the literature, consisting of approximate relations involving the direct correlation functions $c_{ij}(r)$, the interparticle pair potentials $u_{ij}(r)$, and the total correlation functions $h_{ij}(r)$.

The closure relations more frequently used are the so-called mean spherical approximation (MSA), the Percus-Yevick approximation (PY), and the hypernetted chain approximation (HNC). These approximations read [15,18]

$$c_{ij}(r)=-\beta u_{ij}(r), \quad r>\sigma_{ij}\equiv\frac{\sigma_i+\sigma_j}{2}, \quad \text{MSA}, \tag{3.2}$$

where σ_i is the diameter of particles of species i

$$c_{ij}(r)=e^{-\beta u_{ij}(r)}[\gamma_{ij}(r)+1]-\gamma_{ij}(r)-1, \quad \text{PY}, \tag{3.3}$$

$$c_{ij}(r)=e^{-\beta u_{ij}(r)}e^{\gamma_{ij}(r)}-\gamma_{ij}(r)-1, \quad \text{HNC}, \tag{3.4}$$

where $\gamma_{ij}(r)=h_{ij}(r)-c_{ij}(r)$. These closure relations must be consistent with the hard-core condition,

$$h_{ij}(r)=-1, \quad r<\sigma_{ij}. \tag{3.5}$$

Thus, if the pair potentials are known, one can use the O-Z equation and one of these closure relations to obtain the pair correlation functions $g_{ij}(r)$. Here we follow the inverse process. We Fourier transform the O-Z equation to obtain a set of 4 coupled linear equations involving $c_{ij}(k)$ and $h_{ij}(k)$, the Fourier transforms of $c_{ij}(r)$ and $h_{ij}(r)$, respectively. Since we measured $h_{ij}(r)$, we solve the set of equations for $c_{ij}(k)$, which are then transformed back to the real space to get the measured direct correlation functions $c_{ij}(r)$. The pair potentials $u_{11}(r)$ and $u_{12}(r)$ are obtained from $c_{11}(r)$ and $c_{12}(r)$, respectively, using the closure relations above. Here we report the results from the HNC approximation, but the other closure relations lead to qualitatively similar results. The pair potentials determined by this deconvoluting method are presented in Figs. 9 and 10.

Figure 9 shows the results for $u_{11}(r)$. The curve in Fig. 9(a) corresponds to the sample where $n_2^*\approx 0$. Here $u_{11}(r)$ shows a well defined attractive component at around $1.5\sigma_1$. At finite values of n_2^*, $u_{11}(r)$ exhibits also this attractive component at $r\approx 1.5\sigma_1$. As one can see, its position remains basically independent of n_2^* and it becomes only slightly deeper as n_2^* increases. At large concentrations of fixed particles there is an additional feature of the pair potential, namely, the attractiveness of the mobile particles becomes of larger range. One can observe in Fig. 9(c) the development of a second attractive component of $u_{11}(r)$ at larger distances. This second component widens out towards smaller distances and merges with the first attractive well [see Fig. 9(d)]. Thus, one could say that the effective pair potential between the particles of the colloidal liquid exhibits two well

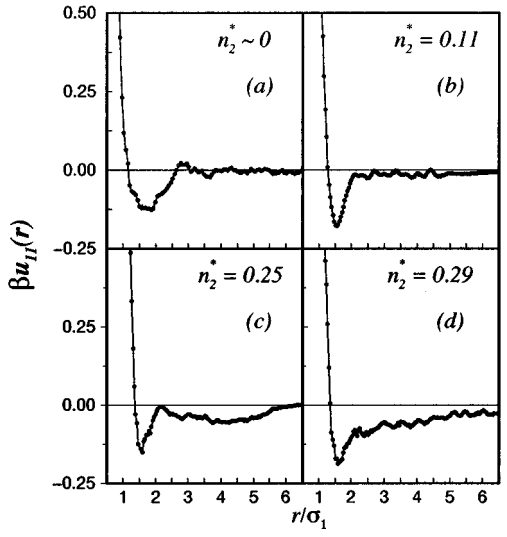

FIG. 9. Effective pair potential between mobile particles in matrices of different porosity.

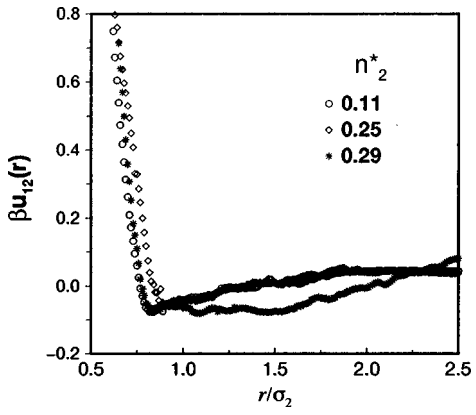

FIG. 10. Effective pair potential between mobile and fixed particles for the samples in Fig. 9.

defined attractive components under the particular confinement studied here. The first attractive component, the minimum at $r \approx 1.5\sigma_1$, can be attributed to the effect of the confining by the glass plates. As shown in Fig. 9 this component changes very little as n_2^* is varied. The second attractive component arises as an extra effect of the fixed particles, which then not only serve as obstacle particles reducing and molding the space available to the colloidal liquid, but their interaction with the mobile particles introduces a strong modification of the effective pair potential $u_{11}(r)$. The other important interaction involved here is the effective interaction potential between the matrix and the mobile colloidal particles, i.e., $u_{12}(r)$. The results for this quantity are shown in Fig. 10. As it turns out, this interaction also happens to be attractive at intermediate distances, which also becomes of longer range as the porosity of the matrix decreases . Since in our systems both species of particles, fixed and mobile, are charged polystyrene spheres, the attractive interaction between them is consistent with the results for $u_{11}(r)$.

In this work we present measurements of the structure of a suspension of charged colloidal particles permeating a model porous medium. Our model system allows us a detailed characterization of both the structure of the colloidal fluid and the matrix. By varying the concentration of the obstacle particles, i.e., the porosity of the matrix, we determine the matrix effect on the structure of the colloidal suspension. According to the results presented here, the strong change of $g_{11}(r)$ observed as a function of n_2^* is a combination of two effects arising from the presence of the obstacle particles. On one hand, the large particles cage the mobile particles within the pores so that they remain close together for longer times than in the homogeneous case ($n_2^* \approx 0$). On the other hand, particles of the matrix also induce changes on the effective interaction between the mobile particles. This interaction is experimentally determined by deconvoluting of the structural function of the system, via the multicomponent O-Z equation. This procedure provides an indirect determination of the effective direct interactions between mobile particles and between them and the particles of the matrix. Although both species are electrically charged with the same sign, we found that under confinement the effective interactions are attractive at intermediate and long distances. These results confirm and advance the notion that the confinement of like charged particles within a charged pore (planar, cylindrical, or other geometries) can induce attractive interactions between the particles. This attractiveness might be due, at least partially, to a nonspherical redistribution of the ionic double layer around the particles caused by the presence of the charged confining walls, as recent calculations show it is the case for a pair of charged particles in a charged cylindrical pore [19]. In the systems studied here, besides the ions dissociated from the surface of the polystyrene spheres, there is a probably large contribution to the ionic strength, and therefore to the screening of the electrostatic interactions, from the ions released from the glass walls [20]. Although both ionic contributions are unknown, one could make a rough estimation of the combined effect by comparing Figs. 2 and 4. As it is seen in these figures, the physical size (Fig. 2) and the effective size as seen by the mobile particles (Fig. 4), of the fixed particles are not much different. Thus, the total ionic concentration must be high enough to provide a Debye screening length smaller than the size of the mobile particles, i.e., smaller that 0.5 μm. Our results also show that the effective potential depends strongly on the confining geometry, at least for the particular system where charged polystyrene spheres are used for both the mobile and the fixed particles. We expect, however, that this simple model system captures the general trends of the physical quantities studied here.

ACKNOWLEDGMENTS

This work was partially supported by the Consejo Nacional de Ciencia y Tecnología, (CONACyT, Mexico).

[1] J. M. Drake and J. Klafer, Phys. Today **43(5)**, 46 (1990).
[2] M. Sahimi, *Flow and Transport in Porous Media and Fractured Rock* (VCH, Weinheim, 1995).
[3] W. G. Madden, J. Chem. Phys. **96**, 5422 (1992).
[4] J. A. Given and G. Stell, J. Chem. Phys. **97**, 4573 (1992).
[5] C. Vega, R. D. Kaminsky, and P. A. Monson, J. Chem. Phys. **99**, 3003 (1993).
[6] G. Viramontes-Gamboa, J. L. Arauz-Lara, and M. Medina-Noyola, Phys. Rev. Lett. **75**, 759 (1995).
[7] G. Viramontes-Gamboa, M. Medina-Noyola, and J. L. Arauz-Lara, Phys. Rev. E **52**, 4035 (1995).
[8] W. B. Russel, D. A. Saville, and W. R. Schowalter, *Colloidal Dispersions* (Cambridge University Press, Cambridge, England, 1989).
[9] P. N. Pusey, in *Liquids, Freezing and Glass Transition*, edited by J. P. Hansen, D. Levesque, and J. Zinn-Justin (Elsevier, Amsterdam, 1991), p. 763.
[10] G. Nägele, Phys. Rep. **272**, 215 (1996).
[11] G. M. Kepler and S. Fraden, Phys. Rev. Lett. **73**, 356 (1994).
[12] M. D. Carbajal-Tinoco, F. Castro-Román, and J. L. Arauz-Lara, Phys. Rev. E **53**, 3745 (1996).
[13] J. C. Crocker and D. G. Grier, Phys. Rev. Lett. **77**, 1897 (1996).
[14] G. Cruz de León, J. M. Saucedo-Solorio, and J. L. Arauz-Lara, Phys. Rev. Lett. **81**, 1122 (1998).
[15] J. P. Hansen and I. R. McDonald, *Theory of Simple Liquids*, 2nd ed. (Academic, New York, 1986).
[16] J. C. Crocker and D. G. Grier, J. Colloid Interface Sci. **179**, 298 (1996).
[17] M. D. Carbajal-Tinoco, G. Cruz de León, and J. L. Arauz-Lara, Phys. Rev. E **56**, 6962 (1997).
[18] D. A. McQuarrie, *Statistical Mechanics* (Harper and Row, New York, 1976).
[19] W. R. Bowen and A. O. Sharif, Nature (London) **393**, 663 (1998).
[20] K. Iler, *The Chemistry of Silica* (Wiley, New York, 1979).